sustainability

Article

Design Optimization of a Root-Targeted Steam Injection Module for Sustainable Thermal Weed Management

Mihai Dan Șerdean [1], Florina Maria Șerdean [2,*] and Silviu Dan Mândru [1]

[1] Faculty of Automotive, Mechatronics and Mechanical Engineering, Technical University of Cluj-Napoca, 103-105 Muncii Blvd., 400641 Cluj-Napoca, Romania; mihai.serdean@mdm.utcluj.ro (M.D.Ș.); dan.mandru@mdm.utcluj.ro (S.D.M.)

[2] Faculty of Industrial Engineering, Robotics and Management Production, Technical University of Cluj-Napoca, 103-105 Muncii Blvd., 400641 Cluj-Napoca, Romania

* Correspondence: florina.rusu@omt.utcluj.ro

Abstract

Sustainable agricultural production requires environmentally friendly weed management solutions. Steam-based thermal weed control is a promising alternative to conventional herbicide-based weed management. However, optimizing steam delivery systems remains computationally expensive due to the repeated simulation-based design evaluations required. This paper presents a design optimization framework for a novel root-targeted steam injection module intended for integration into an autonomous agricultural platform for sustainable thermal weed management. The mechanical behavior of different nozzle geometries was evaluated using finite element analysis using the ABAQUS/CAE software, generating the simulation dataset used for optimization. To reduce the computational cost associated with repeated finite element simulations, a Kriging surrogate model was constructed from this dataset and coupled with an evolutionary optimization algorithm to identify the optimal nozzle geometry. The evaluated nozzle geometries exhibited maximum stresses ranging from 5.12 to 20.41 N/mm^2. The stress value predicted by the Kriging model for the optimized configuration was validated through an additional finite element simulation, showing a deviation of only 6.6%. Furthermore, an artificial neural network model implemented in PyTorch 2.7.1 was trained on the simulation dataset and used as an independent validation tool to estimate the stress corresponding to the optimized nozzle geometry, with a prediction deviating by approximately 5.4% from the corresponding finite element result. The proposed approach significantly reduces computational cost while maintaining high accuracy in stress prediction, enabling the identification of a structurally reliable nozzle geometry for sustainable herbicide-free thermal weed management.

Keywords: sustainable agriculture; thermal weed management; herbicide-free weed control; precision agriculture; design optimization; finite element analysis; surrogate-assisted optimization

Academic Editors: Horațiu Felix Arion and Iulia D. Arion

Received: 26 June 2026
Revised: 12 July 2026
Accepted: 14 July 2026
Published: 20 July 2026

1. Introduction

Sustainable agricultural production requires innovative technologies capable of maintaining high crop productivity while minimizing environmental impact. Among the major challenges in modern agriculture, weeds remain one of the leading causes of agricultural production losses [1]. Conventional weed control methods rely heavily on chemical herbicides, such as clopyralid and metazachlor, which remain among the most widely used but also environmentally controversial agricultural practices. In addition to economic costs, pesticide spraying exposes operators, soil ecosystems, and surrounding wildlife to potentially harmful chemical substances. Recent studies indicate that herbicide usage can alter soil microbial respiration and enzymatic activity, potentially disrupting essential soil processes and affecting long-term crop productivity [2]. Moreover, herbicide production and application may contribute to greenhouse gas emissions and broader environmental challenges [3].

Besides the impact on the environment, the heavy use of chemical herbicides makes agricultural systems vulnerable to rising operational costs, stricter regulations, and the occurrence of herbicide-resistant weeds, such as *Amaranthus palmeri* and *Lolium rigidum*. These aspects further emphasize the need for resilient weed management solutions, preferably based on alternative treatment strategies that reduce chemical dependency while supporting sustainable agricultural systems.

Recent advances in sensing technologies, artificial intelligence, and autonomous navigation have accelerated the adoption of robotic systems in agriculture. Autonomous tractors and mobile robotic platforms equipped with GPS, computer vision, and intelligent decision systems are increasingly being deployed for tasks such as navigation, monitoring, and crop maintenance [4]. The integration of robotic technologies into weed management systems offers significant potential to reduce herbicide usage while improving operational safety and environmental sustainability.

In response to the increasing demand for high crop productivity while minimizing pesticide use, several alternative weed control solutions have been proposed. Some approaches rely on contact-type weed eradication systems designed to reduce herbicide consumption [5]. Other systems combine mechanical and chemical weed removal techniques [6,7], while some focus exclusively on mechanical methods [8]. A notable example is the autonomous robotic platform developed by ecoRobotix, which uses computer vision and robotic actuation to detect weeds and apply precisely targeted herbicide doses [9,10].

Among the alternative approaches, thermal weed control using steam has emerged as a promising sustainable solution. Several studies have demonstrated the effectiveness of soil steaming techniques in suppressing weeds and improving crop yields. For example, the combination of soil steaming, plastic mulching, and winter cover crops has been shown to effectively suppress weeds while enhancing tomato production [11]. Other studies have investigated band steaming, which applies steam to a narrow strip around crop rows to eliminate weed seedlings while minimizing energy consumption [12,13]. Additional approaches combine soil sterilization with mechanical processes such as shredding [14]. Although these methods have demonstrated good weed control performance, most of them rely on surface or near-surface steam application, which may reduce their effectiveness against perennial and deep-rooted weeds and often requires repeated treatments. These limitations highlight the need for root-targeted steam delivery systems capable of directly transferring thermal energy to the root zone of the weeds.

Several existing approaches focus on developing steam-based weed management machines. Most of these are operator-dependent and apply steam only to the surface of the weed [15–20]. In contrast, the solution proposed in this article consists of a novel root-targeted steam injection module that can be mounted on an autonomous platform, enabling direct thermal treatment of weed roots.

The root-targeted steam injection module proposed in this study addresses two major challenges in modern weed management: the high operational costs associated with crop maintenance and the environmental impact of chemical herbicides. The module can be mounted on an existing autonomous mobile agricultural platform and enables the use of pressurized steam as a sustainable and environmentally friendly weed control method. Steam is delivered directly to the weed root through a soil-penetrating injection nozzle,

https://doi.org/10.3390/su18147399

ensuring efficient thermal treatment while minimizing the impact on surrounding crops. By targeting the root zone directly, the proposed solution is capable of treating even deep-rooted weeds, potentially reducing the number of treatment passes required across large agricultural fields and therefore supporting more sustainable agricultural operations.

The proposed thermal weed management system is designed to operate symmetrically on an autonomous mobile platform capable of navigating large agricultural areas and maintaining various crops efficiently. A critical component of this system is the cylindrical soil-penetrating nozzle responsible for delivering steam into the soil. During operation, the nozzle repeatedly penetrates the ground and is subjected to significant mechanical stress. Depending on environmental conditions, such as soil moisture and compaction, the resistance encountered during insertion may vary substantially, increasing the risk of mechanical failure of the nozzle head.

Because the platform is intended to operate autonomously with minimal human supervision, the reliability of the nozzle component is essential. A nozzle failure during field operations may lead to system downtime, increased maintenance costs, and reduced operational efficiency.

To ensure reliable long-term operation, it is therefore necessary to minimize the maximum stress experienced by the nozzle head during soil penetration. Finite element analysis is employed to evaluate the mechanical behavior of different nozzle configurations under realistic loading conditions. However, repeated high-fidelity simulations are computationally expensive, making direct optimization inefficient for large design spaces. Recent studies have shown that surrogate-assisted optimization frameworks can significantly reduce computational cost while maintaining high prediction accuracy in precision agriculture and engineering design applications [21].

This study has two main aims. First, it presents a novel root-targeted steam injection module intended for integration into autonomous agricultural platforms as a sustainable solution for herbicide-free thermal weed management. Second, it optimizes the geometry of the soil-penetrating nozzle through a simulation-driven design methodology in order to minimize the maximum stress generated during soil penetration. To achieve this objective, an evolutionary optimization algorithm is combined with a Kriging surrogate model that estimates stress values for intermediate geometrical configurations, significantly reducing the number of required simulations. In addition, a neural network model trained on the simulation dataset is used to predict stress values for the optimized geometry, providing independent validation of the obtained solution. Through this methodology, the optimized nozzle geometry achieves improved structural reliability and operational durability, supporting sustainable and resilient autonomous agricultural systems.

2. Sustainable Thermal Weed Management System Design

2.1. A Mobile Platform

The proposed innovative steam injector module is the main part of a pressurized steam thermal herbicide autonomous system, which consists of several components.

The largest part of the herbicide system is the mobile platform, which can be even an already existing autonomous mobile platform that combines all elements into a single, autonomous unit capable of moving across various types of plantations. An example of such a platform, designed to maintain two cultivated rows simultaneously, is shown in Figure 1a, whereas Figure 1b illustrates the mounting arrangement of the proposed steam injection module on the autonomous platform. The modular architecture of the proposed system also enables the integration of multiple steam injection units on the same autonomous platform, allowing the working width and field capacity to be adapted according to the specific agricultural application. Depending on the maintenance schedule and the type of crop, the height of the linear guides attached to the platform's legs can be adjusted to ensure they do not interfere with the plants while allowing precise steam injection at the required height.

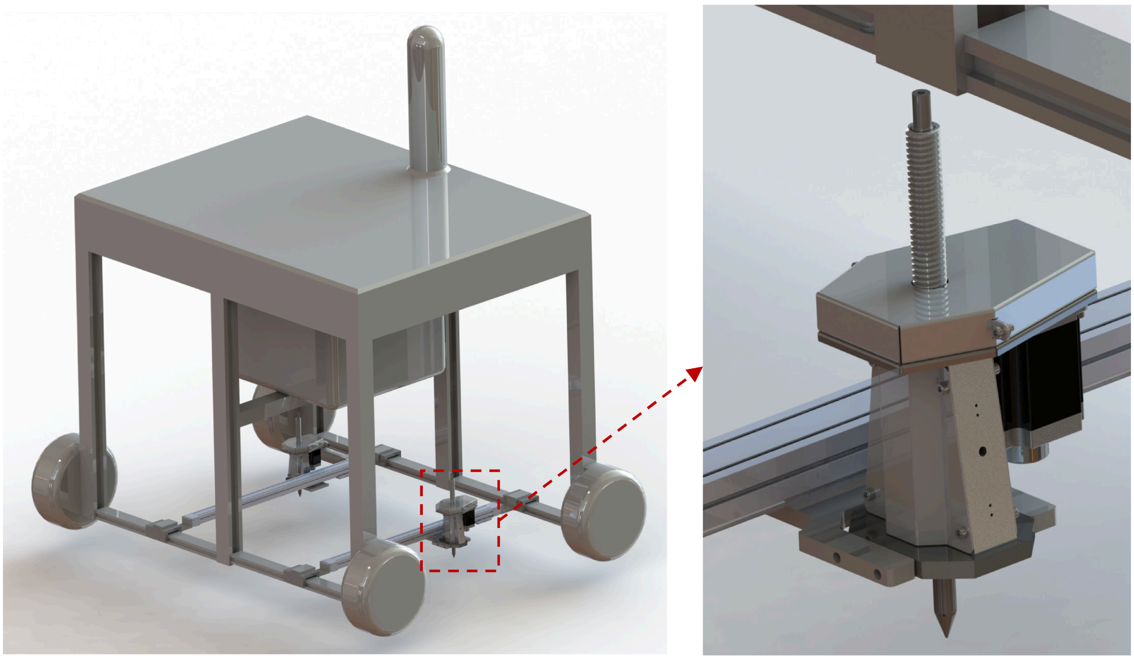

(**a**) (**b**)

Figure 1. (**a**) Example of an autonomous mobile agricultural platform equipped with the proposed root-targeted steam injection module. (**b**) Close-up view of the steam injection module.

The injection device is mounted on a linear guide corresponding to the X-axis. Its primary function is to penetrate the soil and release pressurized steam at the root level of the weeds. Additional details about the design and operation of this injection device, which is the main focus of the present study, are provided in the following section.

The X-axis and Y-axis linear guides enable the injection device to move precisely along these axes, ensuring accurate steam delivery to the detected weeds. These guides are of the electromechanical linear spindle type, equipped with a 3 mm pitch serrated transmission belt (model FESTO EGC-70- -TB-KF), and are driven by a servomotor that provides the required translational movement.

The stand-alone steam generation system proposed for this setup is a compact commercial DHR-8 steam generator powered by an internal combustion engine. The generator uses water as the working medium without chemical additives, producing high-pressure steam that is supplied to the steam injection module through a flexible high-pressure hose. This eliminates the use of chemical herbicides and avoids the release of chemical residues during weed treatment. The steam generator is mounted directly on the autonomous platform and supplies pressurized steam to the injection module during field operation. The system can operate effectively under various weather conditions and offers two operating modes: a low-pressure mode (11–12 bar) with steam temperatures up to 85 °C and a high-pressure mode (80 bar) with temperatures up to 160 °C, allowing adaptation to different soil and weed conditions. The steam generation unit operates independently from the injection module, allowing maintenance, repair, or replacement of the generator without affecting the remaining components of the autonomous platform. Although alternative environmentally friendly steam generation technologies, such as solar- or laser-powered systems, have been reported in the literature, the DHR-8 generator was selected because its compact design facilitates integration into the proposed platform while minimizing the overall system dimensions.

2.2. Steam Injector Module

The primary focus of this study is the optimal mechanical design of the steam injection module responsible for delivering pressurized steam directly to the root zone of weeds. The 3D model was developed using SolidWorks 2019 and is presented in Figure 2.

Figure 2. Three-dimensional model of pressurized steam injection system.

The proposed root-targeted steam injection module is one of the main engineering contributions of this work and is currently the subject of a patent application. Figure 3 presents an exploded view of the module, illustrating its structural architecture, the arrangement of its main mechanical components, the integration of the steam delivery and actuation mechanisms, and the functional relationship between these subsystems.

This representation facilitates understanding of the operating principle of the proposed solution before the structural optimization of the soil-penetrating nozzle is presented in the following sections. The proposed module has overall dimensions of 470 × 195 × 215 mm (height × width × depth), resulting in a compact design suitable for integration into autonomous agricultural platforms. During operation, the steam injection nozzle performs a maximum vertical stroke of 150 mm.

The module consists of three functional subsystems: the supporting structure, which provides mechanical integration with the autonomous platform, the actuation and transmission system, responsible for the vertical movement of the injection nozzle, and the steam delivery system, which transports pressurized steam to the detachable soil-penetrating nozzle.

The supporting structure is built around the base plate 1, which supports all the components of the steam injection module and provides the mechanical interface for mounting the module onto the mobile platform. It also includes two angled support columns 2 connected by a top plate 3, which maintains the correct alignment of the structure while supporting the bearing 4 and the stepper motor 5. The gear transmission assembly is enclosed, and it is protected by a cover plate 6, together with the left cover 7 and the right cover 8.

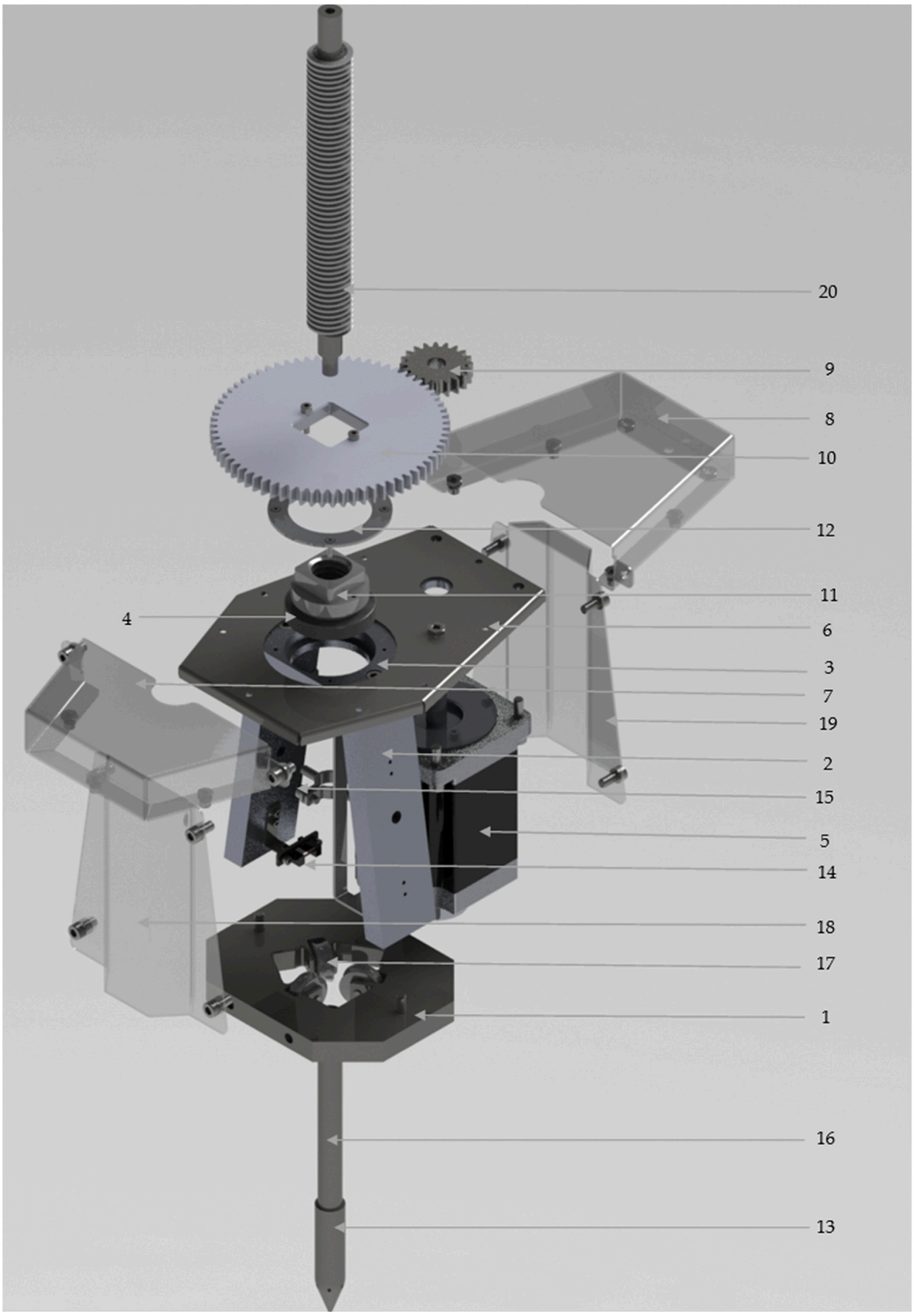

Figure 3. Exploded view of the proposed root-targeted steam injection module illustrating its structural architecture, the main mechanical components, and their assembly (1—Base plate; 2—Support columns; 3—Top plate; 4—Bearing; 5—Stepper motor; 6—Cover plate; 7—Left cover; 8—Right cover; 9—Pinion; 10—Driven spur gear; 11—Custom trapezoidal-thread nut; 12—Circular bearing retainer; 13—Steam injection nozzle; 14—Slotted optical switch; 15—Circular position detection element; 16—High-pressure steam pipe; 17—Pipe guide rollers; 18—Left lower cover; 19—Right lower cover; 20—Custom trapezoidal lead screw).

For this application, a stepper motor NEMA 30 with an encoder was chosen. Motor 5 is mounted at the rear of the injection module, and it is directly connected to top plate 3 and to pinion 9 from the assembly. The driven spur gear 10 is connected to the custom trapezoidal-thread nut 11, which is mounted on the top plate 3 using bearing 4, allowing a smooth rotation motion. Above the top plate, there is a circular cover 12 which locks bearing 4 in place vertically. The nut 11 rotates and thus allows the custom trapezoidal lead screw 20 to move up and down. Part 20 encloses a pipe through which the high-pressure steam can pass all the way to the steam injection nozzle 13. The up and down stroke can be controlled via the encoder of the motor by counting the steps, and with the help of the slotted optical switch 14, which is activated by a circular position detection element 15 mounted on the outside of the high-pressure pipe 16.

Pipe 16 is guided on the lower side by three rollers 17 mounted at 120 degrees in order to prevent any blockages during the up and down movement. The steam injection nozzle 13, which penetrates the soil, is designed to be detachable because it can have different hole patterns for steam ejection, and also, in case it becomes damaged, it can be replaced much easier and more cost-effectively. The lower side is enclosed by the slightly larger lateral left cover 18 and right cover 19, which are bolted directly to support column 2 of the vertical support element.

3. Methods

3.1. Finite Element Analysis for Cylindrical Nozzle

Finite element analysis (FEA) of the soil–nozzle interaction was performed using ABAQUS/CAE v. 6.13-1. The explicit dynamic solver (ABAQUS/Explicit) was used to simulate the penetration process, which involves highly nonlinear contact interactions between the soil and the penetrating nozzle.

In order to perform the finite element analysis in the ABAQUS program, it was necessary to include in the model the characteristics of both interfering bodies, i.e., both the soil characteristics and the penetrating body (of the cylindrical nozzle). Following the study of the literature, several models for the soil were identified according to the mechanical behavior of the soil under the external load of the soil working tool. The Drucker-Prager model and its extended forms are used for modeling frictional materials such as soils and rocks, where the elastic deformation limit of the material is associated with hardening (i.e., the strength of the material increases with the level of stress). The extended forms include a linear, hyperbolic, and general exponential form available in ABAQUS, with the linear form being most suitable for soil materials and used by researchers in their studies. In the analysis carried out in this chapter, soil was modeled as a plastic-elastic material with hardening properties using the linear form of the extended Druck-Prager (ABAQUS/Explicit) model [22].

The model is defined as follows [22]:

$$F = t - ptan\beta - d \tag{1}$$

where F is the function defining the limit of elastic deformation, t is the deviatoric stress, p is the normal stress, b is the internal friction angle, and d is the material cohesion. The normal stress (p) and the deviatoric stress (t) are defined by the following equations:

$$p = \frac{1}{3}(\sigma_1 + \sigma_2 + \sigma_3) \tag{2}$$

$$t = \frac{1}{2}q\left[1 + \frac{1}{K} - \left(1 - \frac{1}{K}\right)\left(\frac{r}{q}\right)^3\right] \tag{3}$$

$$q = (\sigma_1 - \sigma_3) \tag{4}$$

$$r^3 = -(\sigma_1 - \sigma_3)^3 = -q^3 \tag{5}$$

https://doi.org/10.3390/su18147399

where *K* is the ratio of the elastic deformation limits in the tensile stress case and in the compressive stress case in the triaxial test (0.778 <= *K* <= 1).

The validated soil model proposed in [22] was adopted in the present finite element analysis. A homogeneous sandy-clay soil with an average density of 1429 kg/m^3 and a moisture content of 27.24% was considered. The material properties required by the extended linear Drucker–Prager constitutive model, including the elastic parameters, cohesion, internal friction angle, flow characteristics, soil–metal friction coefficient, and pre-compression stress, are summarized in Table 1. The soil was modeled as a parallelepiped with dimensions of 100 mm × 100 mm × 180 mm, which provided sufficient volume to accurately capture the soil–nozzle interaction while limiting boundary effects and maintaining a reasonable computational cost.

Table 1. Soil properties used in the FEM model.

Parameters	Value
Density (g/cm^3)	1.429
Young's modulus, E (KPa)	617
Poisson's coefficient, ν	0.432
Internal friction angle, Mohr-Coulomb φ (°)	13.77
Internal friction angle, Drucker-Prager β (°)	27.34
Flow demand ratio, K	0.85
Angle of expansion, Ψ (°)	0
Cohesion, C (Kpa)	44.814
Soil-to-metal friction coefficient, *f*	0.5
Pre-compression stress, σ_{pc} (KPa)	12.5

The geometry of the penetration nozzle used in the finite element analysis is shown in Figure 4. The nozzle head has a triangular cross-section designed to facilitate soil penetration and reduce insertion resistance. During the optimization process, the nozzle tip angle (*α*) and the nozzle diameter (Ø) were selected as the design variables, while the remaining geometrical dimensions were kept constant. The nozzle is assumed to be made ofAISI 303 stainless steel (EN 1.4305), selected for its good mechanical strength, corrosion resistance, and suitability for repeated exposure to high-temperature steam and condensation during field operation. The material properties used in the finite element analysis are summarized in Table 2.

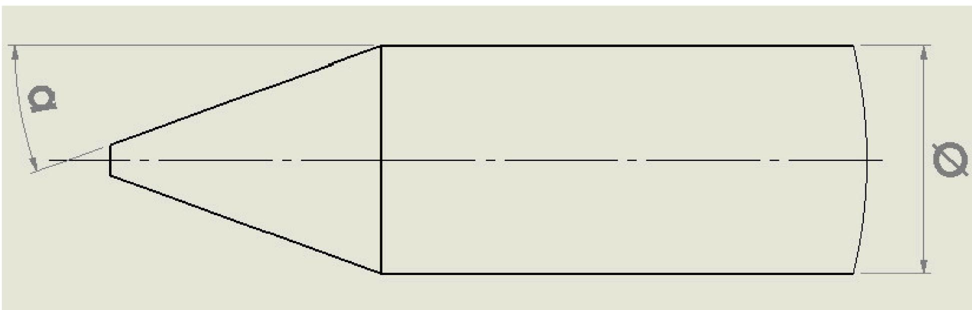

Figure 4. Geometry of the soil-penetrating nozzle showing the design variables considered during the optimization process.

3.2. DACE Toolbox Based on Kriging Interpolation Algorithm

The present finite element analysis focuses on the mechanical stresses generated during soil penetration, which represent the primary loading condition governing the structural design of the nozzle. Thermal stresses and long-term thermal fatigue were beyond the scope of the present study but will be investigated in future work as part of a multi-objective optimization framework.

Table 2. Cylindrical nozzle properties.

Parameters	Value
Density (g/cm^3)	7.9
Young's modulus, E (MPa)	200,000
Poisson's coefficient, ν	0.28
Tensile strength (MPa)	600
Yield strength (MPa)	400

To reduce the computational cost associated with repeated FEA simulations, a surrogate model based on Kriging interpolation was employed. The correspondence between the input data and the Kriging interpolation weights is made using a variogram that illustrates the variance of the difference between measurements obtained at two locations. When compared to other approximation techniques, Kriging has been shown to provide more accurate predictions because it uses correlated errors and recalculates the weights when a new prediction is required. More details on the mathematical model of the Kriging estimator can be found in [23,24].

Kriging has several variations developed, starting from the basic linear regression estimator. Ordinary Kriging is the one that has been used to estimate the maximum stress values for different geometries of the penetration nozzle because this type of Kriging assumes that the mean is constant only in the local neighborhood of each estimation point.

The DACE (Design and Analysis of Computer Experiments) toolbox for MATLAB 2024b is a specialized software package used to facilitate the design and analysis of experiments conducted using computer simulations. It was developed to be used within the MATLAB 2024b environment, and it provides functions and tools for creating and working with surrogate models, particularly Kriging models.

This DACE toolbox was used for assembling a Kriging surrogate model based on the input values for the maximum stress of the penetration nozzle geometries, which allows making predictions for unevaluated nozzle geometries. This toolbox allows users to select regression models with polynomials of zero-, first-, or second-order. Additionally, the correlation model can be selected from seven different models.

The program, developed in MATLAB 2024b using the DACE toolbox, allows the user to provide the input data (different geometries and the corresponding maximum stress) in a file. After reading the data and verifying it, the program develops a design and analysis Kriging model based on the provided data. The model includes normalizing the data, calculating distances, and creating a regression matrix. Using this developed Kriging model, the program predicts the value of the maximum stress for a new penetration nozzle geometry.

The procedure for using this tool consists of the following:

Function Call: maxStress = KrigingTest(inData);
Input: inData—an array containing the geometric parameters of the penetration nozzle to be evaluated;
Output: maxStress—the predicted value of the maximum stress for the given nozzle geometry.

3.3. KGCS Optimization Algorithm

The Cuckoo Search (CS) optimization algorithm draws inspiration from the evolutionary behavior of cuckoo birds, specifically their migratory habits and reproductive strategy. It was developed based on this biological behavior by Xin-She Yang and Suash Deb [25].

The algorithm incorporates Lévy flights, a type of movement observed in nature where animals take seemingly chaotic paths when foraging for food, which involves random step lengths drawn from a Lévy distribution:

$$Lvy \sim u = t^{-\lambda},\ 1 < \lambda \leq 3 \tag{6}$$

This Lévy flight pattern, which occasionally involves significant jumps from the value of the current cuckoo in the k-th generation $x_i^{(k)}$ is used to generate a new cuckoo in the next generation using a scaling factor α, as follows:

$$x_i^{(k+1)} = x_i^{(k)} + \alpha \cdot Lvy(\lambda) \tag{7}$$

The standard CS algorithm, which mimics cuckoo migration using Lévy flights, has been refined to achieve a balanced approach between exploration and exploitation. This evolution led to the development of the KGCS algorithm, which integrates the Knowledge Gradient (KG) policy to manage exploration based on accumulated knowledge.

The KGCS algorithm introduces two distinct phases. The first phase emphasizes exploration of the search space. Here, three populations of cuckoos are initialized with random values within predefined boundaries. Each population independently explores the search space by evaluating its fitness using the objective function. Through multiple generations, cuckoos lay eggs in new nests determined by Lévy flights. At the end of each generation, the best cuckoo from each population is saved in an archive specific to that population. This phase continues until a stopping criterion is met, ensuring thorough exploration of the search space.

After completing 10% of the maximum number of generations, the first phase transitions to the second phase. Using the KG policy, the knowledge gradient values are computed based on the archives containing the best cuckoos from each population. In the second phase, exploitation is prioritized by focusing solely on the population with the highest knowledge gradient value. According to the KG policy, this population is expected to have the greatest potential for advancement. The exploitation phase continues until the maximum allowed number of generations is reached.

The enhanced KGCS algorithm has been rigorously tested on various benchmark functions and has been applied successfully to solve optimal design problems [26,27]. This adaptation demonstrates the algorithm's effectiveness in balancing exploration and exploitation to achieve optimal solutions in computational optimization scenarios. Therefore, this enhanced algorithm was used to reach the objective of the optimization process, namely, to minimize the maximum stress experienced by the nozzle head during soil penetration.

3.4. Artificial Neuronal Network Model

To provide an additional data-driven estimation of the stress values associated with different nozzle geometries, a feedforward artificial neural network (ANN) was implemented in Python using the PyTorch 2.7.1 deep learning framework. The complete dataset used for training consisted of 16 finite element simulations generated from the ABAQUS finite element analyses performed for multiple geometric configurations of the nozzle. The input variables consisted of the nozzle diameter (Ø) and the penetration angle (α), while the output variable corresponded to the maximum stress obtained from the simulations. The input variables covered the same design space considered during the optimization process, with the nozzle diameter ranging from 10 to 25 mm and the cone angle ranging from 10° to 40°.

The neural network architecture consisted of two input neurons, two fully connected hidden layers with 10 neurons each, and a single output neuron. The network architecture was selected empirically to provide sufficient nonlinear approximation capability while avoiding unnecessary model complexity, considering the limited size of the available dataset. Rectified Linear Unit (ReLU) activation functions were applied to the hidden layers to introduce nonlinearity, while the output layer remained linear in order to perform regression. The model was trained using supervised learning with the mean squared error (MSE) loss function and the Adam optimizer with a learning rate of 0.01 for 10,000 training epochs.

To evaluate the predictive capability of the neural network, one simulation case was excluded from the training dataset and used as an independent verification sample. The predicted maximum stress differed by 5.8% from the corresponding finite element result, demonstrating good agreement between the ANN estimation and the numerical simulation. Considering the limited size of the available dataset, resulting from the high computational cost of the finite element simulations, the ANN was employed primarily as an auxiliary data-driven verification tool rather than as a standalone predictive model. After training, the network was used to estimate the maximum stress corresponding to the optimized nozzle geometry, which was not included in the training dataset and was obtained through the surrogate-assisted optimization framework.

3.5. Optimization Framework

The overall optimization framework adopted in this study is illustrated in Figure 5. The proposed optimization framework combines finite element simulations, surrogate modeling, and an evolutionary optimization algorithm. First, a set of nozzle geometries is evaluated using FEA simulations to obtain the corresponding maximum stress values. These simulation results are then used to train a Kriging surrogate model capable of estimating stress values for intermediate geometries. The KGCS algorithm uses this surrogate model to efficiently explore the design space and identify the geometry that minimizes the maximum stress. Finally, the optimized geometry is validated through additional FEA simulations and neural network-based stress prediction.

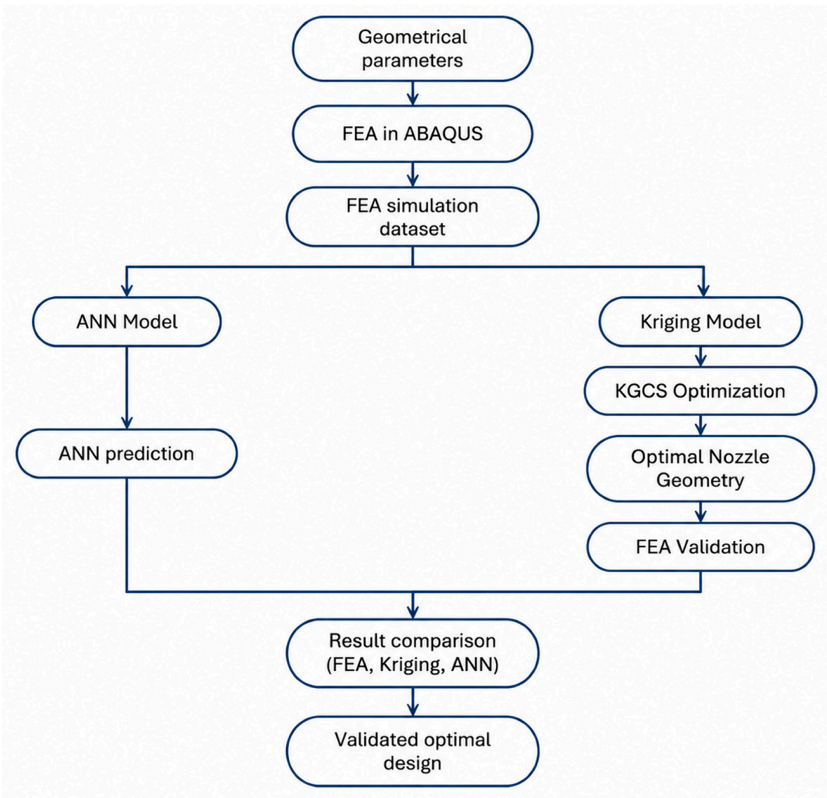

Figure 5. Workflow of the proposed optimization framework for nozzle geometry design.

4. Results and Discussion

This section presents the results of the optimization process aimed at determining the optimal design of an herbicide-free weed management constructive solution, namely, determining the optimal geometry of a penetration nozzle that ensures a minimum stress on the nozzle in order to maximize its life.

4.1. ABAQUS Finite Element Analysis

The first step consisted of performing the finite element analysis in the ABAQUS program. Initially, the 3D interaction model was developed in SolidWorks 2019, and the .step files were imported into ABAQUS. Then, for more flexibility in terms of simulation and modification of nozzle values (angle and diameter), the model was also developed in ABAQUS using the dedicated toolbox. The created model consisted of two distinct parts: a deformable soil and a rigid model nozzle. The discretization density has a large influence on the simulation run time, along with other factors such as penetration depth, angle, nozzle diameter, and other specific parameters that are related to the ABAQUS program.

The 3D model for the soil was created as a deformable type, and for the nozzle as a discrete rigid type. The material properties, such as density, elasticity, or plasticity, for both soil and penetration nozzle were chosen according to Tables 1 and 2. Subsequently, the section was created, and it was attached to each individual component.

Both bodies were positioned in the assembly so that they were ready for the penetration simulation stage. In this case, the interaction between the soil and the nozzle was modeled with a tangential surface-to-surface contact layer using the penalty function method. Also at this stage, the value of the friction coefficient 0.5 is introduced, taking into account the material types chosen for both the soil and the penetration nozzle. The modeling of this interaction can be observed in Figure 6.

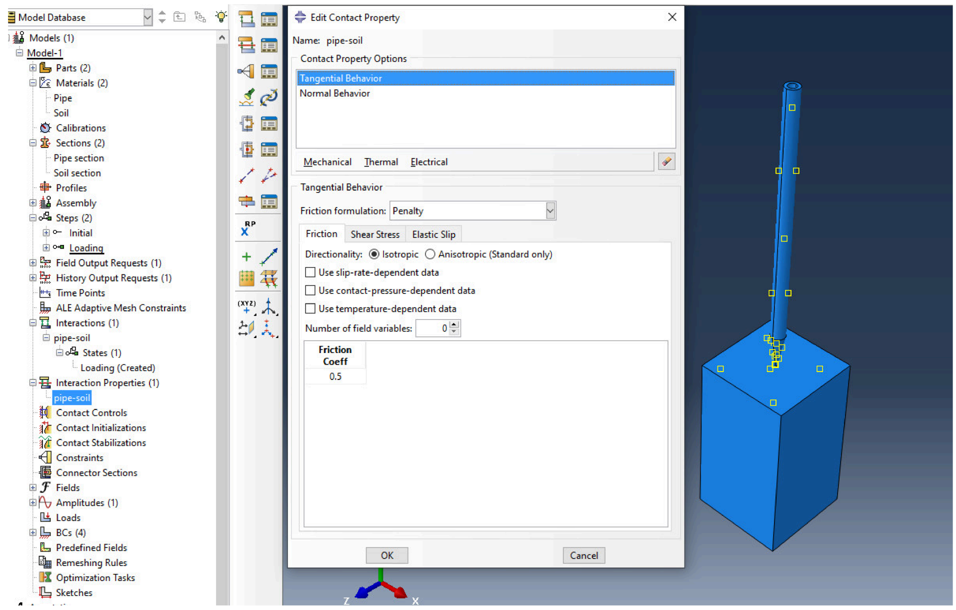

Figure 6. Establishing interactions between components in ABAQUS/CAE v. 6.13-1.

The chosen type of interaction is given not by setting the penetration force, but by setting a penetration depth that varies between 60 mm and 150 mm, the maximum limit being taken from the specialized literature. According to studies carried out, in automated plantation maintenance, soil sterilization with specialized machines is performed for the first 150 mm [28].

The discretization of the bodies is achieved by choosing the appropriate type of element and dividing the soil and nozzle model into finite elements. For both the soil and the nozzle, mesh sizes were chosen experimentally by the trial-and-error method. It was observed that the mesh size considerably influences the running time of the soil penetration simulation. However, it was necessary to determine a value small enough to minimize the running time but, at the same time, large enough to eliminate erroneous results as well as artifacts during the visualization of the penetration. Following simulations with several discretizations, it was concluded that their optimal values are different for the two bodies. Depending on the mesh and penetration depth, the duration of a simulation ranged from two days to two weeks.

The maximum von Mises stresses obtained from the finite element simulations for all combinations of nozzle diameter and cone angle are summarized in Table 3. A total of 16 nozzle geometries were evaluated within the selected design space. As can be seen, the results indicate that the maximum stress on the nozzle tip can increase by almost four times depending on the selected geometry. This variation confirms that the nozzle geometry has a significant influence on the mechanical response during soil penetration. Furthermore, the nonuniform distribution of stress values across the design space indicates a nonlinear relationship between the geometric design variables and the resulting stresses, further justifying the use of surrogate-assisted optimization techniques. To better illustrate the stress distribution and the interaction between the soil and the penetration nozzle, ABAQUS was used to generate sectional ("View Cut") visualizations of the simulated model. A representative example is presented in Figure 7, highlighting the location of the maximum stress for a given nozzle geometry.

Table 3. Results of the simulations performed in ABAQUS.

Ø \ **α**	**10°**	**20°**	**30°**	**40°**
10 mm	8.30 [N/mm^2]	6.71 [N/mm^2]	12.86 [N/mm^2]	9.32 [N/mm^2]
15 mm	8.12 [N/mm^2]	5.88 [N/mm^2]	5.60 [N/mm^2]	5.12 [N/mm^2]
20 mm	16.84 [N/mm^2]	7.17 [N/mm^2]	7.47 [N/mm^2]	6.21 [N/mm^2]
25 mm	14.03 [N/mm^2]	6.84 [N/mm^2]	20.41 [N/mm^2]	13.61 [N/mm^2]

4.2. Optimal Penetration Nozzle Geometry

The second step consisted of determining the optimal geometry for the penetration nozzle. Due to the long computational time required for performing a simulation in ABAQUS of the interaction between a penetration nozzle and the soil, and based on the results of the performed simulations, the Kriging interpolation technique has been used to approximate the maximum stress on the nozzle with a geometry for which a simulation in ABAQUS has not been performed.

The geometry for the penetration nozzle was previously shown in Figure 4, and the parameters indicated there are considered as unknowns in the optimization problem formulated in this subsection. The purpose is to find the best values for the geometric parameters that will minimize the maximum stress when inserting the nozzle in the soil. Thus, the problem is formulated as a minimization problem:

$$\min_{\alpha, Ø} \sigma_{max}(\alpha, Ø) \tag{8}$$

where

$$\sigma_{max} : [\alpha_{inf}, \alpha_{sup}] \times [Ø_{inf}, Ø_{sup}] \to (0, \infty) \tag{9}$$

$$\alpha_{inf} = 10,\ \alpha_{sup} = 40,\ Ø_{inf} = 10,\ Ø_{sup} = 25 \tag{10}$$

This optimization problem was solved using the KGCS algorithm described in Section 3.3. The optimization process begins by generating three initial populations of 100 cuckoos, where each cuckoo represents a nozzle geometry defined by the pair (α, $\varnothing$). The fitness of each possible solution is evaluated using the Kriging surrogate model generated based on the dataset presented in Table 3. The surrogate model with a first-order polynomial regression model and a cubic correlation model was identified as the most suitable for accurately predicting the maximum stress values of unevaluated nozzle geometries.

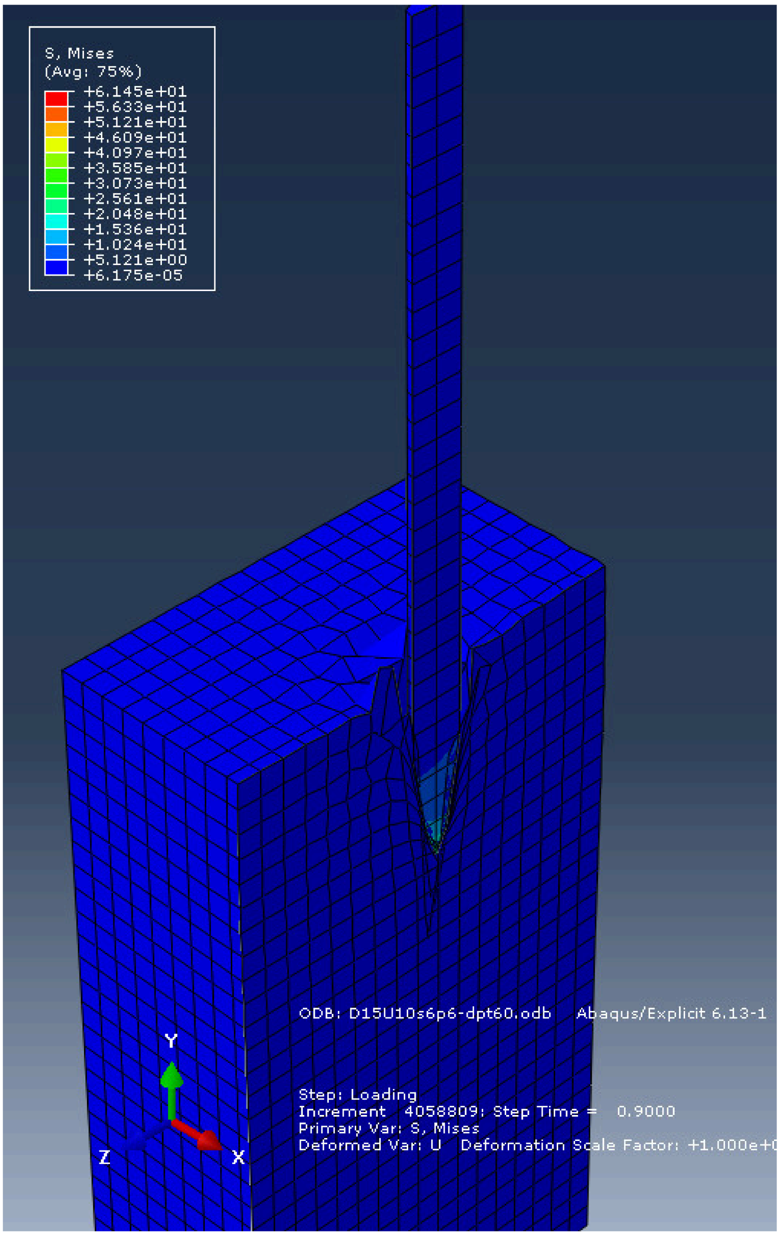

Figure 7. Example of simulation results in ABAQUS/CAE v. 6.13 − 1.

During the exploration phase, new possible solutions are generated using Lévy flights, ensuring the exploration of the design space while continuously updating the best solutions in each population archive. After 5% of the maximum number of iterations, the knowledge gradient is computed for each population, and the population with the highest value is selected for the exploitation phase. The search then focuses on the most promising region of the design space until convergence, with the best cuckoo representing the optimal nozzle geometry that minimizes the maximum stress during soil penetration. Running the optimization for 90,000 objective function evaluations took three seconds. This time justifies the use of a surrogate model instead of the finite element analysis method, which took on average three days for a single evaluation using ABAQUS.

The pair of optimal values for the geometrical parameters obtained from the optimization is given by the angle $\alpha\_optimal$ = 31.46° and the diameter $\varnothing\_optimal$ = 17.22 mm. For easier manufacturing and taking into account that there is no significant difference between the maximum stress obtained with the values α_optimal and $\varnothing\_optimal$ and the maximum stress obtained with α = 31° and $\varnothing$ = 17 mm, the optimal values can be rounded to 31° and 17 mm, respectively.

The maximum stress on the nozzle head for the geometric configuration given by the optimal solution was also calculated using the finite element method in the ABAQUS software, resulting in a value of 5.082 [N/mm^2]. Compared to the estimated value of 4.748 [N/mm^2], a difference of approximately 6.6% was observed.

To further verify the robustness of the obtained optimization results, a feedforward neural network was developed using the PyTorch 2.7.1 framework to provide an independent prediction of stress values. The network was trained using the dataset obtained from the ABAQUS simulations, with the geometric parameters of the nozzle serving as inputs and the corresponding maximum stress values as outputs.

The trained neural network was then used to estimate the stress value for the optimized nozzle geometry (α = 31°, $\varnothing$ = 17 mm). The trained neural network predicted a maximum stress of 4.81 N/mm^2 for the optimized nozzle geometry, corresponding to a deviation of approximately 5.4% from the finite element result (5.082 N/mm^2). This prediction is also in close agreement with the estimate obtained using the Kriging surrogate model, further supporting the reliability of the proposed optimization framework. The predicted maximum stress was 4.81 N/mm^2, which is in close agreement with both the Kriging surrogate model estimate and the finite element simulation results. The consistency of the predicted stress values obtained using these three independent approaches indicates the reliability of the optimized design and confirms the suitability of surrogate modeling techniques for reducing the computational cost associated with repeated finite element simulations during the early stages of mechanical design. It should be noted that the ANN was not intended to serve as a standalone predictive model. Since only a limited number of finite element simulations were available for training, the network was used exclusively as an auxiliary verification tool. Consequently, the ANN was assessed based on its prediction errors for both the independent verification case and the optimized nozzle geometry, rather than on conventional machine learning performance metrics, such as RMSE and R^2.

Overall, the combination of Kriging interpolation, evolutionary optimization, finite element analysis in ABAQUS, and neural network prediction provided an efficient and consistent framework for nozzle design optimization. The obtained nozzle geometry minimizes the maximum stress experienced during soil penetration while maintaining structural integrity during repeated operation. This improves the mechanical reliability and durability of the root-targeted steam injection module, reducing maintenance costs and improving the efficiency of long-term operations of autonomous thermal weed systems.

5. Conclusions

The increasing demand for sustainable and efficient agricultural production highlights the need for alternative weed management solutions that reduce labor costs and minimize the environmental impact of chemical herbicides. In this work, a novel root-targeted steam injection module intended for integration into autonomous agricultural platforms was developed as an environmentally friendly solution for sustainable thermal weed management. The proposed modular concept provides a practical foundation for precise steam delivery directly into the root zone of weeds while supporting future large-scale autonomous field operation. Since the soil-penetrating nozzle is the most mechanically demanding component of the proposed system due to its repeated insertion into the soil, its geometry was selected for optimization.

The proposed optimization framework successfully identified a nozzle geometry that minimizes the maximum mechanical stress generated during soil penetration while substantially reducing the number of computationally expensive finite element simulations required during the design process. The optimized solution predicted by the Kriging surrogate model was confirmed through an additional finite element simulation, showing a deviation of only 6.6%. Furthermore, the independent ANN verification predicted the stress for the optimized geometry with a deviation of 5.4% from the finite element result, further demonstrating the robustness and accuracy of the proposed methodology.

The optimized nozzle geometry improves the structural reliability of the steam injection module by reducing the maximum stress generated during operation. From a practical perspective, this improvement is expected to increase component durability, reduce maintenance frequency and operational downtime, and enable the use of cost-effective materials without compromising structural integrity. Furthermore, the proposed root-targeted steam delivery concept contributes to herbicide-free weed management and supports the development of more sustainable agricultural systems.

A limitation of the present study is that the optimization was performed exclusively under mechanical loading conditions using numerical simulations. Consequently, the effects of repeated thermal loading on the nozzle and the experimental performance of the complete system were beyond the scope of the present work.

Future work will focus on the experimental validation of the proposed root-targeted steam injection module through laboratory and field tests under real operating conditions. These experiments will be used to validate the numerical predictions presented in this study, evaluate the effectiveness of the proposed thermal weed management approach for different weed species and soil conditions, and assess the long-term reliability of the system after integration into an autonomous agricultural platform.

6. Patents

The mechanical concept of the proposed steam injection module is currently submitted to OSIM; the patent application number is A00287/07.07.2025.

Author Contributions: Conceptualization, F.M.Ș., M.D.Ș. and S.D.M.; methodology and supervision, S.D.M.; software, F.M.Ș. and M.D.Ș.; validation and data curation, F.M.Ș. and M.D.Ș.; formal analysis and writing—original draft preparation, F.M.Ș. and M.D.Ș.; writing—review and editing, F.M.Ș., M.D.Ș. and S.D.M.; visualization, F.M.Ș. and M.D.Ș. All authors have read and agreed to the published version of the manuscript.

Funding: This research received no external funding.

Institutional Review Board Statement: Not applicable.

Informed Consent Statement: Not applicable.

Data Availability Statement: The original contributions presented in this study are included in the article. Further inquiries can be directed to the corresponding author.

Acknowledgments: The authors would like to thank the Technical University of Cluj-Napoca, Romania, for providing technical support in conducting the research.

Conflicts of Interest: The authors declare no conflicts of interest.

Abbreviations

The following abbreviations are used in this manuscript:

CS	Cuckoo Search
KGCS	Knowledge Gradient Cuckoo Search
FEA	Finite Element Analysis
DACE	Design and Analysis of Computer Experiments

References

1. Rathika, S.; Udhaya, A.; Ramesh, T.; Shanmugapriya, P. Weed management strategies in green gram: A review. *Pharma Innov. J.* **2023**, *12*, 5574–5580.
2. Rouhi-Kelarlou, T.; Golchin, A.; Soltani Toularoud, A.A. Ecotoxicological impact of butisanstar and clopyralid herbicides on soil microbial respiration and enzymatic activities. *Chemosphere* **2024**, *357*, 142029. [CrossRef] [PubMed]
3. Cornish, C.M.; Johnson, O.F.; Bansal, S.; Meier, J.A.; Harris, T.D.; Sweetman, J.N. Common use herbicides increase wetland greenhouse gas emissions. *Sci. Total Environ.* **2024**, *933*, 172881. [CrossRef] [PubMed]
4. Soleimani, A.; Abbaspour-Fard, M.H.; Sapkota, R.; Sanaeifar, A. Artificial intelligence in agricultural machinery & robotics: A systematic review and future outlook. *Appl. Soft Comput.* **2026**, *194*, 114889. [CrossRef]
5. Chandel, A.K.; Tewari, V.K.; Kumar, S.P.; Nare, B.; Agarwal, A. On-the-go position sensing and controller predicated contact-type weed eradicator. *Curr. Sci.* **2018**, *114*, 1485–1494. [CrossRef]
6. Bawden, O.; Kulk, J.; Russell, R.; McCool, C.; English, A.; Dayoub, F.; Lehnert, C.; Perez, T. Robot for weed species plant-specific management. *J. Field Robot.* **2017**, *34*, 1179–1199. [CrossRef]
7. Jiang, W.; Quan, L.; Wei, G.; Chang, C.; Geng, T. A conceptual evaluation of a weed control method with post-damage application of herbicides: A composite intelligent intra-row weeding robot. *Soil Tillage Res.* **2023**, *234*, 105837. [CrossRef]
8. Averill, K.M.; Westbrook, A.S.; Pineda-Bermudez, L.; O'Briant, R.P.; DiTommaso, A.; Ryan, M.R. Effects of Tertill® weeding robot on weed abundance and diversity. *Agronomy* **2022**, *12*, 1754. [CrossRef]
9. EcoRobotix. Weeding Robots Startup ecoRobotix Raises CHF 10.6 Million, 2018. Available online: https://www.startupticker.ch/en/news/may-2018/ecorobotix-raises-chf-10-6-million-in-series-b-financing (accessed on 30 January 2026).
10. EcoRobotix. Steve Tanner (Long Pitch)—EPFL Alumni SeedNight/Innovaud, YouTube Video. Available online: https://www.youtube.com/watch?v=tiyLSOCwX5c (accessed on 30 January 2026).
11. de Oliveira, T.R.; Serafim, A.D.; Breland, B.; Miller, A.; Beneton, K.; Singh, V.; Segbefia, W.; Argenta, J.C.; Broderick, S.R.; Tseng, T.M. An integrated weed management approach in tomato using soil steaming, mulching, and winter cover crops. *Front. Agron.* **2023**, *5*, 1075726. [CrossRef]
12. Guerra, N.; Fennimore, S.A.; Siemens, M.C.; Goodhue, R.E. Band steaming for weed and disease control in leafy greens and carrots. *HortScience* **2022**, *57*, 1453–1459. [CrossRef]
13. Kristensen, E.F.; Jørgensen, M.H.; Kristensen, J.K. Intra-Row Weed Control by Use of Band Steaming. Available online: https://orgprints.org/id/eprint/10005/1/10005.pdf (accessed on 3 January 2025).
14. Kim, Y.S. Eco-friendly Hot Steam Soil Sterilizer with Soil Shredder. U.S. Patent US11785896B2, 2023.
15. Kerpauskas, P.; Sirvydas, A.P.; Lazauskas, P.; Vasinauskiene, R.; Tamosiunas, A. Possibilities of weed control by water steam. *Agron. Res.* **2006**, *4*, 221–225.
16. Lipes, A. Manually Controlled and Operable Self-Propelled Seed Bed Sterilization System and Method to Prevent Weeds. U.S. Patent US20210227757A1, 25 October 2022.
17. Railway Technical Research Institute. Weed Control Nozzle. Japan Patent JP2022205246A, 17 August 2023.
18. Shim, D.S.; Park, S.D. Portable Weed Removing Device Using Steam. Korea Patent KR20110103148A, 20 September 2011.
19. Cristiano, B.; Sartorato, D.; Friso, D.; De Zanche, C.; De Paoli, F.; Bietresato, M. Weed control by water steam using a self-propelled machine equipped with a condensation chamber. *Agric. Eng. Int. CIGR J.* **2010**, *12*, 1–10.
20. Langshaw, E. Hot Water/Steam Weed Killing System. U.S. Patent US5385106A, 31 January 1995.
21. Cheng, D.; Yao, Y.; Liu, R. Precision agriculture management based on a surrogate model assisted multiobjective algorithmic framework. *Sci. Rep.* **2023**, *13*, 1142. [CrossRef] [PubMed]
22. He, C.; You, Y.; Wang, D.; Wang, G.; Lu, D.; Kaji, M.T. The effect of tine geometry during vertical movement on soil penetration resistance using finite element analysis. *Comput. Electron. Agric.* **2016**, *130*, 97–108. [CrossRef]
23. Rusu, F.; Tudose, L.; Tudose, C. Bearing life approximation using Kriging. *Acta Tech. Napoc. Ser. Appl. Math. Mech. Eng.* **2015**, *58*, 219–224.
24. Crișan, H.G.; Șerdean, F.; Bîrleanu, C.; Pustan, M.; Crișan, O.A. An efficient method for testing the quality of drinking-water filters used for home necessities. *Int. J. Environ. Res. Public Health* **2022**, *19*, 4085. [CrossRef] [PubMed]

25. Yang, X.S.; Deb, S. Cuckoo search via Lévy flights. In *Proceedings of the World Congress on Nature & Biologically Inspired Computing (NaBIC)*; IEEE: New York, NY, USA, 2009; pp. 210–214.
26. Tudose, L.; Rusu, F.; Tudose, C. Optimal design under uncertainty of bearing arrangements. *Mech. Mach. Theory* **2016**, *98*, 164–179. [CrossRef]
27. Șerdean, F.M.; Șerdean, M.D.; Mândru, S.D. Maintenance cost minimization for an agricultural harvesting gripper. *Sensors* **2023**, *23*, 4103. [CrossRef] [PubMed]
28. Peruzzi, A.; Raffaelli, M.; Ginanni, M.; Fontanelli, M.; Frasconi, C. An innovative self-propelled machine for soil disinfection using steam and chemicals in an exothermic reaction. *Biosyst. Eng.* **2011**, *110*, 434–442. [CrossRef]

https://doi.org/10.3390/su18147399